

Electron energy distribution functions in processing plasmas

N. St.J. Braithwaite

Materials Discipline, Faculty of Technology, The Open University, Walton Hall,
Milton Keynes, MK7 6AA, U.K.

ABSTRACT

The electron energy distribution function (EEDF) in a low pressure processing discharge is a good indicator of the state of the plasma. Chemical kinetics are especially sensitive to the EEDF and the electron population plays a central role in coupling power into the desired surface reactions. Process development and transfer will be aided by a knowledge of the EEDF and its sensitivity to various process parameters.

The EEDF can be measured using an electrostatic probe to sample the electron population by drawing a small current from the plasma. Electron and ion density and a characteristic electron (Maxwellian) temperature can be deduced from probe data. Furthermore, the current-voltage characteristic of the probe represents integrated EEDF information which can be recovered by differentiation. The practical use of this probe technique is considered for a variety of plasmas (both DC and RF generated). The problems associated with processing plasmas such as deposition and RF excitation are discussed with particular emphasis on 13.56MHz capacitively coupled systems. Typical data are viewed in terms of energy resolution and accuracy and conditions necessary for reliable data acquisition are considered.

1 INTRODUCTION

EEDF in low pressure processing plasmas

The Electron Energy Distribution Function (EEDF) in a low pressure processing plasma is very much a 'fingerprint' of the discharge. In these media (pressures up to a few torr, and charged particle density 10^{14} - 10^{17} m^{-3}) the electron population is characterised typically by a temperature (or mean energy) of a few electron volts (eV). The electrons are not in thermal equilibrium with the gas and its ions (which are generally much cooler than the electrons) and the electron temperature which describes the bulk of the electron distribution does not necessarily extend into the tail.

It is through the electrons that electrical energy is principally coupled to the plasma (the ions and the gas). Ionisation is almost entirely dependent on electron impact and in simple gases the excitation is similarly exclusive. In molecular gases, although the situation is much more complicated through the wide variety of species (and energy states within each one) the distribution of electron energies is still an important indicator of what processes have or could have taken place. For example in nitrogen discharges, the EEDF can show significant depletion around 3eV where there is a large cross-section for vibrational excitations of the gas molecule (refs. 1,2). Over distances comparable with the mean free path for inelastic processes, there can be significant variation of the EEDF, reflecting for example changes in the composition of the medium (refs. 3-5). The chemical kinetics of processing plasmas are very sensitive to details of the EEDF.

In discharges sustained by radio frequency (RF) fields a further complication arises in connection with the temporal behaviour of the EEDF. In a plasma carrying an RF conduction current, the EEDF must necessarily show some variation during the RF cycle, and the amount will depend upon the ratio of the drift to the random electron flux. This ratio can be estimated from the RF current density, j , and the random charge flux ($ne_c/4$). For example, suppose 100W of RF power is supplied as 700 V (amplitude) and 280 mA (amplitude) of in phase current to a discharge between parallel plates (diameter 0.2 m). Taking account of additional displacement currents which are at least comparable, the plasma current may be around 1 A and the current density about 30 Am^{-2} . For a plasma density of 10^{15} m^{-3} and an electron temperature of 2 eV, the random charge flux would be about 120 Am^{-2} . In this case, the current may cause a significant time variation in the EEDF (see also ref. 2).

Figure 1 shows the result of a measurement of the EEDF in a 13.56 MHz argon plasma. Data points clearly depart from the pure Maxwellian trend indicated by the solid line and there is distinct structure to the data. In fig. 1(a) the EEDF is presented on a linear scale showing the number density per unit of energy range ($dn/d\epsilon$)

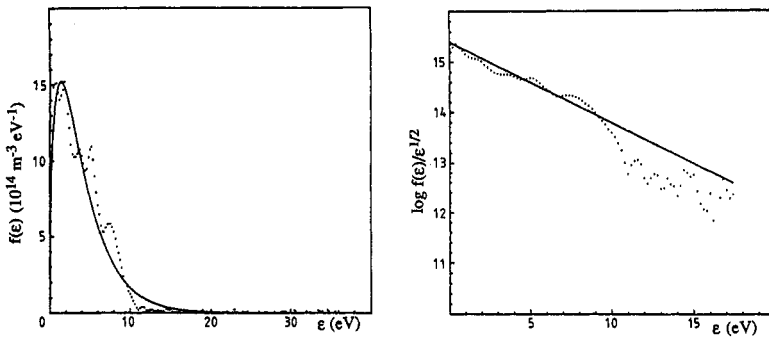


Fig. 1. Measured EEDF for a 100W, 13.56MHz argon plasma .

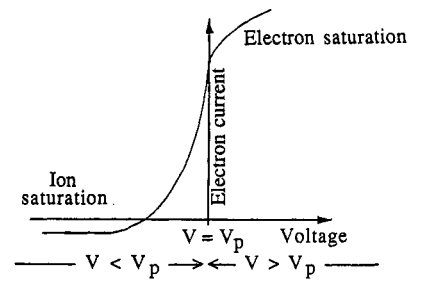


Fig. 2. Schematic $I(V)$ characteristic for a single probe.

against energy (ϵ). In fig. 1(b) there is a logarithmic plot of part of the EEDF which conveniently shows Maxwellian distributions as straight lines and which is readily generated by the experimental measurement. In this review I want to discuss how to obtain results like that in fig. 1 and to investigate what confidence we should have in them. To do this it is necessary to consider details of the experimental technique which uses an electrostatic probe. This will be done starting with the principle of the method and examples of EEDF measurements in DC plasmas. Then the environment of processing plasmas which introduces reactive gases and/or RF will be considered.

2 PROBES, CURRENTS AND THE EEDF

There are several satisfactory accounts of electrostatic plasma probes which detail the collection processes for charged particles (refs.6-8). Probe methods will in principle permit the spatially resolved measurement of charged particle densities and energies.

In this section the principle of the electrostatic probe and its use in measuring the EEDF will be described, briefly. The EEDF is recovered from the electron current to the probe which is an integral over the related velocity distribution.

The Langmuir probe

The charged particle population of a gas discharge may be sampled by drawing a current between a pair of electrodes immersed in the plasma. The perturbation caused by these 'probe' electrodes must either be slight or else properly accounted for in interpreting data from such a system. The current flow between two probe electrodes is in general a function of the local plasma conditions and the electrode geometry as well as the externally applied potential.

By using asymmetrical probe electrodes it is possible to concentrate changes in the applied potential to a non-neutral space charge sheath region around the smaller probe so that its local conditions are the more dominant. This arrangement provides the so-called single Langmuir probe. In its simplest form, a single probe is just a small disk, wire or sphere of conductor, used in conjunction with a much larger, reference electrode furnished by a convenient conducting surface exposed to the same plasma, such as one of the discharge electrodes. This is the configuration of most interest in obtaining data on the electron energy distribution.

The ratio of probe to reference electrode area must be much less than the square root of the electron to positive ion mass ratio, $(m/M)^{1/2}$. This criterion is based upon the requirement for the reference electrode to be able to collect positive charges at the same rate of coulombs per second as the probe may collect electrons, but without a significant shift in potential of the reference with respect to the plasma, as the probe current varies.

The current-voltage relation for a single probe

Figure 2 shows a schematic current-voltage characteristic for a single Langmuir probe in a typical low pressure plasma. There are three regions indicated which are distinguished by the nature of the collected current - just electrons at large positive potential, just ions at large negative potential and a mixture in between.

Consider first the intermediate region in which the probe is at a more negative potential than the plasma which is adjacent to it. Negative charges (electrons and negative ions) will only reach the probe surface if they have sufficient energy to overcome the adverse potential. By contrast, positive charges will be accelerated towards it (the basis of ion-assisted surface processes).

At sufficiently large negative potential, the current flow to the probe will be due solely to positive ions - termed saturated positive ion collection or 'ion saturation current'. The magnitude of the current may still go on

increasing through geometric effects as the influence of the more negative potentials extend further into the surrounding medium, though not as a strong function of potential (ref.6).

The opposite extreme of positive bias and negative charge collection is ostensibly similar, although the thermal energy of electrons is markedly more than that of the ions and this can adjust the detail of the saturation region. Also, in low pressure plasmas the positive ions usually have insufficient thermal energy to reach the probe once its potential has become positive. In the absence of negative ions, this situation is referred to as the electron saturation region.

The characteristic can be conveniently summarised algebraically by writing the components of current as functions of the potential difference between probe and plasma:

$$I(V) = I_+(V) \quad V \ll 0 \quad (1)$$

$$I(V) = I_+(V) + I_{\text{-ret}}(V) \quad V \leq 0 \quad (2)$$

$$I(V) = I_{\text{-acc}}(V) \quad V > 0 \quad (3)$$

For the present it is sufficient only to study the detail of the intermediate regime where electrons are retarded and positive ions are accelerated as they approach the probe. The EEDF can be extracted from differentials of the electron component of this probe current.

For the simple case of a Maxwellian electron energy distribution characterised by a temperature T , the retarded electron saturation current is given by:

$$I_{\text{-ret}}(V) = Aen\sqrt{\frac{kT}{2\pi m}} \exp(eV/kT) \quad (V < 0) \quad (4)$$

where A is the probe area, n the plasma density, k is Boltzmann's constant, e is the magnitude of the electronic charge and m is the electron mass.

The EEDF and retarded electron current

If the EEDF were Maxwellian then it follows from equation (4) that a graph of $\log_e(I_{\text{-ret}})$ against $-V$ would yield a straight line of slope e/kT . This is usually the first test that is carried out on probe data - departures from a linear semi-log plot being indicative of a non-Maxwellian EEDF. It is often the case that the bulk of the characteristic fits the Maxwellian description sufficiently well for some representative temperature to be ascribed to the electrons. Departures in the tails of distributions are not uncommon.

A complete Maxwellian is not expected owing to the non-equilibrium nature of low pressure discharges. For instance, in filament assisted discharges or those in which secondary emission from electrodes plays a crucial role, there may be a non-thermal tail comprising electrons scattered from an initial beam. In some cases the probe data is better fitted by a 'two temperature' distribution with hotter and colder components having distinct densities (n_h, n_c) and temperatures (T_h, T_c). In this case equation (4) is changed to:

$$I_{\text{-ret}}(V) = Ae[n_h\sqrt{\frac{kT_h}{2\pi m}} \exp(eV/kT_h) + n_c\sqrt{\frac{kT_c}{2\pi m}} \exp(eV/kT_c)] \quad (5)$$

and again the semi-log plot allows first T_h and after extrapolation T_c to be extracted. Andreu *et al* (ref. 9) have reported a case where three sources of electrons (ionization, hot filament and secondary emission) was well fitted by the sum of three Maxwellians.

Not all distributions fit these Maxwellian based approximations. Furthermore, detailed modelling of molecular gases is very sensitive to the structure of the EEDF so it is important to be able to probe the EEDF directly.

It was shown by Mott-Smith and Langmuir (ref. 10) that an *isotropic* EEDF could be recovered from the second differential with respect to potential of the retarded electron current for planar, cylindrical or spherical collecting probes. Druyvesteyn (ref. 11) later showed that the result applies to any convex probe shape and the technique is now often referred to as the Druyvesteyn method. In the retardation region the probe acts as an energy filter only receiving particles of sufficient initial kinetic energy to overcome the adverse potential. The retarded electron current can therefore be expressed in terms of $F(\epsilon)$ the velocity distribution remote from the probe (in plasma undisturbed by the presence of the probe), taking account of all possible combinations of angles of incidence and energy (see ref. 6):

$$I_{\text{-ret}}(V) = \frac{Ae}{2\sqrt{2m}} \int_{-eV}^{\infty} (\epsilon + eV) \epsilon^{-1/2} F(\epsilon) d\epsilon \quad (6)$$

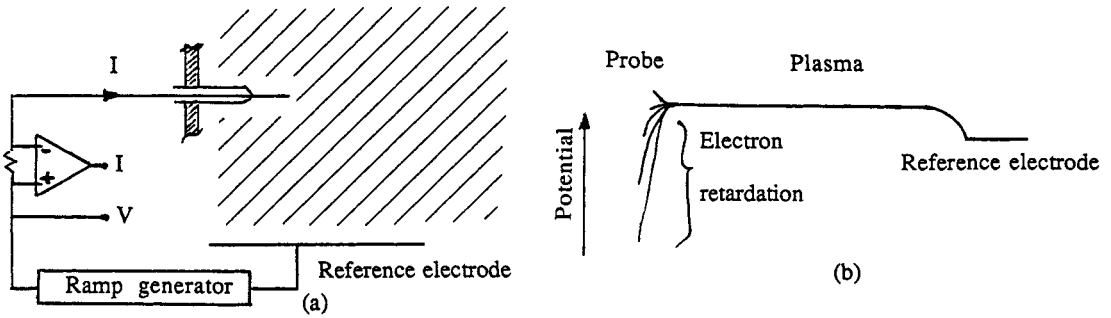


Fig. 3. (a) Circuit diagram for a single probe characteristic.
 (b) Schematic of the distribution of potential around the circuit in 3(a).

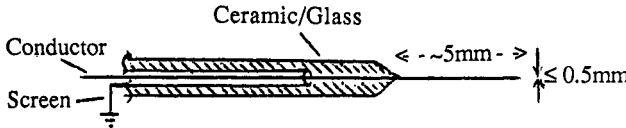


Fig. 4. Construction of a single probe.

Differentiating with respect to voltage involves both the integrand and the limits with the result that after two differentiations (with $\epsilon \equiv -eV$):

$$d^2I_{ret}/dV^2 = \frac{e^3 A}{4} \sqrt{\frac{2}{m(-eV)}} F(-eV). \tag{7}$$

The EEDF can therefore be recovered from the retarded electron component of the probe data. The skill in using this relationship to measure real distribution functions lies in obtaining two differentiations of real data without too much degradation of the resolution and of the signal to noise ratio.

In presenting the data it is often convenient to display the second derivative directly as the combined function $F(\epsilon)/\epsilon^{1/2}$ is a simple exponential for a Maxwellian energy distribution since

$$F_{Maxwellian}(\epsilon) = dn_{Maxwellian}/d\epsilon = \frac{2}{\pi^{1/2}} n (kT)^{-3/2} \epsilon^{1/2} \exp(-\epsilon/kT). \tag{8}$$

3 EEDF MEASUREMENTS

The single probe characteristic

Figure 3(a) shows a circuit diagram for measuring the $I(V)$ characteristic for a single probe. Figure 3(b) shows how the potential is distributed around the circuit. In the laboratory, the probe potential is V_{bias} , conveniently referred to the larger electrode, but the theory uses the undisturbed plasma as the zero of potential so that the probe potential with respect to the plasma is V , as illustrated in the figure. The characteristic changes abruptly in passing from electron retardation to electron acceleration - the knee in the curve therefore locates the plasma potential which is needed to establish the proper origin of the retardation current data. Plasma potential is the origin of the energy scale.

The construction of a single probe is shown in fig. 4. Further details can be found in standard texts such as refs.6 and 8.

Techniques for obtaining the EEDF

The EEDF is bound up in the retarded electron current. It is necessary to differentiate this current twice with respect to voltage and to identify the plasma potential which is the proper zero of the energy scale.

The double differentiation of real signals is not of itself difficult provided the signals are unusually noise free and smooth. Whereas integration smoothes changes essentially diminishing the higher frequency components, differentiation accentuates changes by enhancing the higher frequency content. In practice therefore, it is necessary to limit the effective bandwidth or to sample and average to maintain a high enough signal to noise ratio. There are several ways in which the current signal can be differentiated.

Early techniques used a small ac modulation of the probe signal to differentiate it. The principle is based upon a Taylor expansion as follows: (the prime denotes differentiation.)

$$I(V + \delta V) = I(V) + \delta V I'(V) + \frac{1}{2} \delta V^2 I''(V) + \dots \tag{9}$$

The simplest modulation is $\delta V = v \cos \omega t$ whereupon the current is given by

$$I(V + v \cos \omega t) = I(V) + I'(V)v \cos \omega t + \frac{1}{2} I''(V)v^2 \cos^2 \omega t + \dots, \quad (10)$$

The first derivative is proportional to the amplitude of the fundamental and this can be used in conjunction with a second, numerical differentiation to establish the EEDF (ref. 12). Alternatively, expanding the $\cos^2 \omega t$ term reveals a component at 2ω (ref. 13) and a small dc shift (ref. 14) both of which are proportional to the second derivative. Other modulation schemes have also been used. The resolution can be no larger than the amplitude of the modulation ($\Delta \epsilon \geq ev$).

Another way of differentiating the probe current is to use operational amplifiers to derive a second differential with respect to time. If the probe potential is swept linearly with time the result is proportional to the desired voltage differential since:

$$\frac{d}{dt} = \frac{dV}{dt} \frac{d}{dV}. \quad (11)$$

This approach in practice needs careful high frequency filtering to avoid swamping the signal with noise enhanced by the differentiation (ref. 15). Here the resolution is limited by the sweep rate and the upper cut-off frequency, f_{\max} so $\Delta \epsilon \geq (e/f_{\max}) dV/dt$.

A third method (refs. 16,17) uses analogue circuitry to perform a finite difference algorithm (eqn. (9)) to infer the second derivative in real time. A repetitive sweep of the probe allows sampling and averaging techniques to increase the signal to noise ratio. The size of the voltage increment limits resolution ($\Delta \epsilon \geq e\delta V$).

The present fashion is to record digitised probe data and afterwards use numerical methods (finite difference and curve fitting algorithms) to smooth and to differentiate the signals (refs. 3, 18-20). Again sampling and averaging gives useful noise compensation. The resolution depends on the number of data points and the type of smoothing algorithm, but is comparable with other methods. The real advantage of the digital method is that it allows the reatrded electron current to be separated form the ion current which is simultaneously collected. Extrapolating from far into the ion saturation region using suitable models of ion collection (e.g. refs 6-8) enables data to be obtained with minimal distortion due to $d^2 I_+(V)/dV^2$.

4 PARTICULAR PROBLEMS FOR PROCESSING PLASMAS

Deposition onto probes and supports

The introduction of a small probe electrode into a processing plasma exposes it to a medium which is intended to modify surfaces. Thus the surfaces of the probe (and its support) may be etched or coated by different material through etching sputtering or CVD. However, conditions at the probe surface may well be different from those which favour the processes destined for the 'workpiece', and there is a good chance that the probe can be made to function. For example, if the probe is held at a large negative bias when not in use then sputtering by ion bombardment will help to keep the probe clean between the taking of data. The possible slow erosion of a probe by ion-assisted etching mechanisms is a desirable side-effect of the non-ideal environment. Clean probes are essential to good quality data. The other extreme of drawing a large electron saturation current is also useful for cleaning, heating the probe ohmically to red heat but it does cause a much greater perturbation to the plasma (removing electrons at a high rate) and also the hot surface may well promote CVD reactions.

Mosburg, Kerns and Abelson (ref. 21) found that in a silane deposition plasma (13.56 MHz), silicon deposition onto the probe tip was inevitable but not a problem. They deduced that there was sufficient optically (and thermally) activated conductivity across the deposited layer to allow probe currents to flow virtually unimpeded. Other work in silane (a hot cathode DC discharge, ref. 20) found no problem with deposition onto the probe provided the vacuum chamber was heated to above 200°C. In a 27MHz silane and hydrogen plasma Bruno *et al.* (ref. 22) noted no difficulty in operating an electrostatic probe. The major concern with conducting deposits is that they will eventually lead to a drastic increase in probe area when material deposited on insulating supports eventually connects with material on the probe.

Insulating films are a real hazard to electrostatic probing. Halogenated hydrocarbon plasmas for example can coat probe electrodes (as well as other surfaces) with polymeric material, the presence of which renders the probe useless. Such layers take time to form and might be kept at bay by biasing the probe to a large negative potential except when data is being recorded (each data point need only take a fraction of a millisecond). Rayment and Twiddy (ref. 4) used repetitive sampling pulses of only 10 μsec to establish the EEDF in a neon DC discharge. They were concerned to obtain time resolved data but the same pulsed method was used to prevent a probe from melting (avoiding prolonged electron saturation) in a higher current neon discharge (ref. 23) and could be used to advantage in avoiding insulating deposits in reactive media.

Effects of RF potential fluctuations

There are two sources of RF potential fluctuations in the plasma which interfere with probe data. The first is 'noise' due to the waves and instabilities in the plasma. Low pressure laboratory plasmas are not in thermal equilibrium, they have gradients of density and temperature, they may be sustained by beams of energetic (ionizing) electrons all of which can enhance the noise. The second source arises for systems excited by RF power. In these, the plasma potential may fluctuate in synchronism with the applied RF voltage. The discussion concentrates on capacitively coupled discharges.

There is little one can do about incoherent broadband noise, which in the end limits the resolution achievable with probe methods (refs. 24-26). However if the noise is limited to a few hundred kHz then some compensation is possible by subtracting the signal from a second nearby probe which senses only fluctuations of the floating potential (refs. 27-30).

The occurrence of coherent fluctuations of plasma potential can in some way be accommodated. Unless action is taken to eliminate or otherwise account for RF voltage between the probe and the plasma, the resolution of average probe data will be limited to the RF amplitude. For useful EEDF results the RF must be reduced to much less than the mean energy.

There are three bands of frequency to be considered: 'low' frequency in which ions and electrons in the plasma are affected; 'intermediate' frequency in which ion inertia restricts the effects to the electrons; 'higher' frequencies which are too fast even for the plasma electrons. The characteristic response frequencies of ions and electrons in a plasma of density n are given respectively by

$$\omega_{pi} = \sqrt{\frac{ne^2}{M\epsilon_0}} \quad \text{and} \quad \omega_{pe} = \sqrt{\frac{ne^2}{m\epsilon_0}},$$

so these frequency bands are $\omega < \omega_{pi}$, $\omega_{pi} < \omega < \omega_{pe}$ and $\omega_{pe} < \omega$. In the third band the probe senses only averaged effects and this case will not be considered further.

Low Frequency. For argon ions at a density of 10^{15} m^{-3} the low frequency range extends up to 1MHz. There may be some variation of plasma parameters (space potential, density and electron temperature or EEDF) during the RF cycle in this range; Anderson *et al.* (ref. 31) for example found at least a factor of two variation in density and temperature in a 100kHz argon plasma. The extraction of the EEDF and the general use of probes in these circumstances needs phase-locked sampling of the probe signal so that measurements are made with respect to a single value of plasma potential and density. In fact, for the apparatus of Anderson *et al.*, the plasma potential was reckoned not to follow the applied RF voltage throughout the cycle, having more the shape of a sine wave severely clipped on one side. Measurements were restricted to instants in the half-period corresponding with the steady value of the plasma potential. The EEDF was obtained with almost microsecond resolution (ref. 1), but of course the ion response frequency (ω_{pi}) also limits the reaction time of the probe which in this case was also around one microsecond. Adriaansz (ref. 16) demonstrated a time resolved technique in a 1kHz square wave modulated discharge in a mercury-neon mixture at 10 torr; a resolution of a few microseconds was achieved. Rayment and Twiddy (ref. 4) examined the evolution of the EEDF through the ionization waves in a 0.35 torr neon discharge with similar resolution.

In low pressure systems where the dominant loss process is wall recombination, reduction of the plasma density is limited by the speed at which ions can be dragged to the walls by the electrons. Rarefaction fronts will propagate through the plasma in a time which is much longer than the reciprocal ion plasma frequency, ω_{pi}^{-1} (ref. 32), so the density may not show much modulation near or above this frequency.

Intermediate Frequency. 13.56 MHz systems usually fall into this category. The use of probes in this regime has to contend with space potential fluctuations which electrons follow but which are too fast for the ions. In addition, the plasma perturbation by the probe is made worse by the loading effect of the capacitance to ground of the probe circuitry. For a fixed probe making relative measurements, the capacitive loading by the probe may be tolerable but it must be avoided if the probe is to be used to obtain spatial variations.

Both passive and active techniques have been developed to allow probes to be used in this intermediate regime. The passive methods attempt to use a resonant filter just behind the probe tip so that at the frequency of the dominant fluctuation the probe presents a very high impedance. At much lower frequencies a low impedance path exists so that probe voltages can be applied and modulated at a few kHz (see fig. 5). The RF blocking impedance has to work with a probe which typically collects tenths of an amp per square metre for voltage changes of about one volt around the zero current point (floating potential) - this is based on a 2eV, 10^{15} m^{-3} plasma. For a 5mm diameter one sided disc-shaped probe (area is $2 \times 10^{-5} \text{ m}^2$) the probe voltage would change by about 0.5 V/ μA near floating potential and the blocking impedance should be much larger than 0.5 M Ω ($\approx 0.5 \text{ V}/\mu\text{A}$).

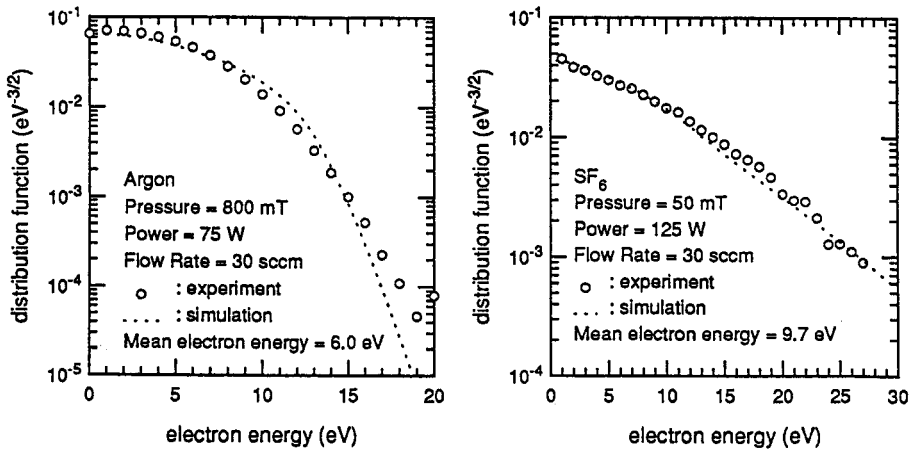


Fig. 5. Measured and calculated EEDFs in argon and sulphur hexafluoride

Several authors have used this approach. Gagne and Cantin (ref. 33) working at 3.5MHz found it helpful to incorporate a second LC filter to block the second harmonic of the RF in the plasma. It is difficult to make small, simple passive networks for higher frequencies but Godyak and Popov (ref. 34) claim to have operated such a circuit at 40MHz and later (ref. 35) EEDFs taken with this probe system were reported. The difficulty with a fixed circuit is that there is no direct indication of its satisfactory operation. Ivanov *et al.* at 2.4GHz (ref. 36) and Paranjpe *et al.* at 13.56MHz (ref. 37) were able to tune their blocking impedance while monitoring the floating potential of the probe. Since RF potentials across the single probe sheath depress the floating potential (refs. 25,26), optimal tuning corresponds with the most positive (or least negative) floating voltage.

In this way the RF block can be 'seen' to be having some beneficial effect. EEDFs have been measured using passive RF blocks (refs. 35-37). The agreement with numerically simulated EEDFs for RF plasmas in argon and in sulfur hexafluoride is reasonably good over a range of 3kT of energy (see fig. 5).

It would be useful to know just what value of impedance is achieved in practice by these passive circuits, since it is not obvious that the probe sheath is without residual RF potential. Indeed, Cantin and Gagne (ref. 38) found it necessary to add to their 3.5 and 7MHz filters the noise suppression technique of actively subtracting the floating potential fluctuation of a second probe, claiming that then less than 0.1V of RF remained across the sheath.

Not surprisingly, treating the applied RF as 'noise' to be nulled works at low frequency too (ref. 39) but at higher frequency the demands on the sense amplifier are severe - not only must it have a high input impedance and be mounted behind the probe tip (to avoid cable loading) but it must also have a flat gain and phase response if it is to work with anything except a pure sine wave. Since the plasma potential fluctuates because of the applied RF, there is no need to sense the fundamental frequency of the disturbance this is available directly from the oscillator; also the amplitude and phase of any compensating signal in the probe circuit can be optimised using the maximal floating potential condition. So the second (sense) probe can be omitted. This is the principle of the RF driven probe technique (refs. 23,32) for which the circuit is illustrated in fig. 6.

The Data in fig. 1 were recorded using this system with numerical processing of digitised data. As in all these RF probe methods, energy resolution may be set by the residual, uncompensated RF potential across the probe sheath, so it is valuable to have some information on just what remains. If the plasma potential were to fluctuate as a pure sine wave then there need be no residual RF but plasma sheaths are not linear circuit elements. The use of a matching network to couple a low impedance generator to a non-linear plasma load

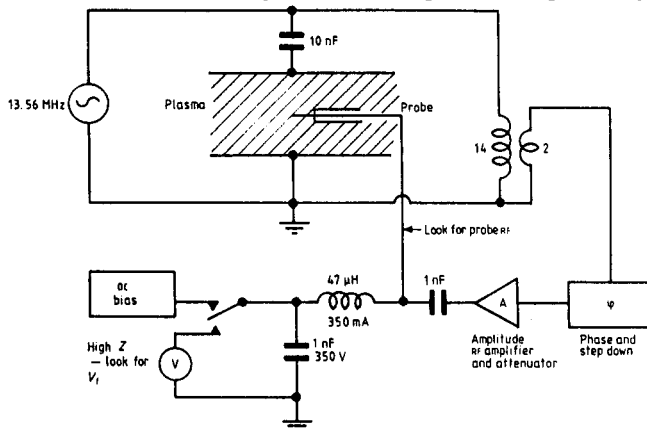


Fig. 6. The RF-driven probe.

may compound the problem leading to non-sinusoidal voltages across the excitation electrodes. The shape of the plasma potential fluctuation need not necessarily be a pure sinusoid and may well also depend on factors such as electrode areas. Nevertheless, recent measurements by Wilson *et al.* indicate a surprisingly pure potential waveform in the plasma. This could be an artefact of their system which loads the plasma with the cable capacitance of two undriven probes (ref. 40). Yet it cannot be missed that the tuned RF probes, both active and passive, all clearly show an optimal condition so at least some of the RF is eliminated. The provision of compensation for at least some of the harmonics may be the prudent means of gaining further credibility.

CONCLUSION

Returning to the data of fig.1 for an RF argon plasma, it is now clear that the energy resolution remains uncertain. Numerical smoothing over a few data points limits resolution to no better than 1eV. Any uncompensated RF in excess of this will further degrade the resolution, and unrealistic extrapolation of the ion current could further impair the fidelity of the data. This makes it especially difficult to probe the higher energies, although a surface mounted energy filter has proved useful here (ref. 41). Where plasmas also include beams of say secondary electrons (e.g. ref. 13) or when the geometry leads to large ratios of drift to random flux then the environment may be insufficiently isotropic to merit the classical analysis in full (ref. 42).

Nevertheless, the intrusion of the probe provides valuable information with regard to process reproducibility if nothing else. Improved analysis and interpretation will follow from the continued use of this basic diagnostic.

A valuable complement to this articles is provided by ref. 43.

REFERENCES

1. M.B.Hopkins, C.A.Anderson and W.G.Graham, Europhys. Lett **8**, 141-145 (1989).
2. M.Capielli, R.Celiberto, C.Gorse, R.Winkler and J.Wilhelm, J. App. Phys **62**, 4398-4403 (1987).
3. M.B.Hopkins and W.G.Graham, Rev. Sci. Instr. **57**, 2210-2217 (1986).
4. S.W.Rayment and N.D.Twiddy, J. Phys.D: Appl Phys **2**, 1747-1754 (1969).
5. V.Godyak, R.Lagushenko and J.Maya, Phys Rev A **38**, 2044-2055 (1988).
6. J.D.Swift and M.J.R.Schwar, Electrostatic probes for plasma diagnostics, Iliffe, London (1970).
7. P.M.Chung, L.Talbot and K.J.Touryan, Probes in stationary and flowing plasmas, Springer-Verlag, New York (1975).
8. F.F.Chen, Electric Probes in Plasma diagnostic techniques, Ed. R.H.Huddlestone and S.L.Leonard, Academic press, New York (1965).
9. J.Andreu, G.Sardin, J.Esteve and J.L.Morenza, J.Phys.D: Appl Phys. **18** 1339-1345 (1985).
10. H.H.Mott-Smith and I.Langmuir, Phys Rev **28**, 727-763 (1926).
11. M.J.Druyvesteyn, Z.Phys. **64**, 781-798 (1930)
12. R.L.F.Boyd and N.D.Twiddy, Proc. R. Soc. **250A**, 53-69 (1959).
13. D.Andersson, J. Phys D: Appl Phys **10**, 1549-1556 (1969).
14. R.Sloan and E.I.R. MacGregor, Phil Mag **18**, 193-207 (1934).
15. K.F.Schoenberg, Rev. Sci. Instr. **49**, 1377-1383 (1978).
16. M.Adriaansz, J.Phys.E: Sci. Instrum. **6**, 743-745 (1973).
17. K.Shimizu and H.Amemiya, J.Phys.E: Sci. Instrum. **10**, 389-391 (1977).
18. T.I.Cox, V.G.I.Deshmukh, D.A.Hope, A.J.Hydes, N.St.J.Braithwaite and N.M.P.Benjamin, J.Phys.D: Appl Phys **20**, 820-831 (1987).
19. D.Maundrill, J.Slatte, A.I.Spiers and C.C.Welch, J.Phys.D: Appl Phys **20**, 815-819 (1987).
20. J.Andreu, G.Sardin, A.Lloret, J.Esteve and J.L.Morenza, J. Appl Phys. **63**, 1230-1232 (1988).
21. S.W.Rayment and N.D.Twiddy, J. Phys D: Appl Phys **6**, 2242-2249 (1973).
22. G.Bruno, P.Capezuto, G. Cicala and F.Cramarossa, Proc. 8th E C Phot. Solar Energy Conf. **2**, 1641-1643 (1988)
23. E.R.Mosburg, R.C.Kerns and J.R.Abelson, J. Appl Phys. **54**, 4916-4927 (1983).
24. V.A.Godyak and S.N.Oks, Sov. Phys Tech Phys **24**, 784-785 (1979).
25. A.Boschi and F.Magistrelli, Nuovo Cimento **29**, 487-499 (1963).
26. A.Garscadden and K.G.Emeleus, Proc Phys Soc. **79**, 535-541 (1962).
27. S.S.Gulidov, Y.M.Kagan, N.B.Kolokolov and V.M.Melenin, Sov Phys Tech Phys **14**, 993-994 (1970).
28. Y.M.Kagan, N.B.Kolokolov, R.I.Lyagushchenko, V.M.Melenin and A.M.Mirzabekov, Sov Phys Tech Phys **16**, 561-564 (1971).
29. S.Matsumura and Sin-Li Chen, Rev. Sci. Instr. **50**, 1425-1428 (1979).
30. H.M.Musal, J. Appl Phys. **41** 2605-2609 (1970).
31. C.A.Anderson, W.G.Graham and M.B.Hopkins, Appl. Phys. Lett **52**, 783-785 (1988).
32. N.St.J.Braithwaite, N.M.P.Benjamin and J.E.Allen, J.Phys.E: Sci. Instrum. **20**, 1046-1048 (1987).
33. R.R.J.Gagne and A.Cantin, J. Appl. Phys. **43**, 2639-2646 (1972).
34. V.A.Godyak and O.A.Popov, Sov Phys Tech Phys **22**, 461-464 (1977).
35. V.A.Godyak and S.N.Oks, Sov Phys Tech Phys **24**, 1255-1256 (1979).
36. Y.A.Ivanov, Y.A.Lebedev and L.S.Polak, Sov Phys Tech Phys **21**, 830-833 (1976).
37. A.P.Paranjpe, J.P.McVittie and S.A.Self, submitted to J. Appl. Phys. (1989).
38. A.Cantin and R.R.J.Gagne, Appl. Phys. Lett **30**, 316-319 (1977).
39. M.B.Hopkins, A.P.Hughes, J.C.Molloy and J.V.Scanlan, Le Vide, les Couches Minces, **246Supp**, 308-310 (1989).
40. J.L.Wilson, J.B.O.Caughman, P.L.Nguyen and D.N.Ruzic, J.Vac.Sci.Tech. A **7**, 972-976 (1989).
41. S.G. Ingram and N. St.J. Braithwaite, J. Phys. D.: Appl. Phys **21**, 1496-1503
42. J.E. Allen, J. Phys. D: Appl. Phys **11**, 135-136 (1978)
43. V.A. Godyak, NATO ASI (Plasma surface interaction and processing of materials) Spain (1988)